Macromolecules

pubs.acs.org/Macromolecules Article

Polyelectrolyte Gels: Swelling and Deswelling upon Nonlinear Deformations

Zilu Wang, Yuan Tian, and Andrey V. Dobrynin*

Cite This: *Macromolecules* 2023, 56, 6543−6551 Read Online

ACCESS | Metrics & More | Article Recommendations | Supporting Information

ABSTRACT: Polyelectrolyte gels, made by crosslinking of ion-containing polymers, showcase extraordinary swelling capabilities, with their volumes expanding up to 100 times in salt-free solutions. This swelling behavior of polyelectrolyte gels is attributed to the delicate balance between the gels' elasticity and the osmotic pressure produced by counterions and salt ions localized within the gel volume due to the Donnan equilibrium. We use a combination of the nonlinear version of Flory−Rehner theory and coarse-grained molecular dynamics simulations to explore the swelling and deformation of polyelectrolyte gels undergoing large biaxial deformations in contact with a salt solution. The analysis of the gel deformation points out that the swelling ratio of the polyelectrolyte gels Q_{eq} describing the volume change upon swelling is a nonmonotonic function of the gel deformation ratio α characterizing changes in a gel shape under biaxial deformation with respect to a free-standing swollen state. The swelling ratio first increases with increasing α and then starts to decrease. This intriguing behavior is due to the optimization of osmotic pressure and conformational entropy of charged strands in the nonlinear deformation regime. Furthermore, we observe that the location of the maximum swelling ratio shifts toward large gel deformations with increasing salt concentration and decreasing fraction of the charged groups on network strands. This behavior is a direct result of the reduced influence of the ions' osmotic pressure on strand prestretching in the free-standing gels.

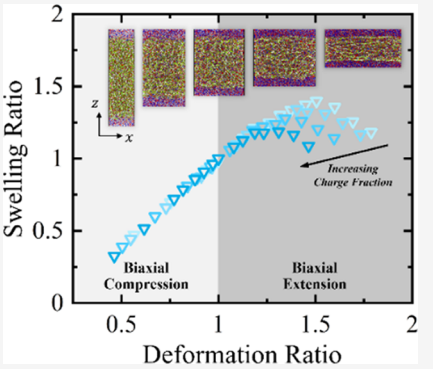

INTRODUCTION

Polyelectrolyte gels, made by crosslinking linear chains with ionizable groups (Figure 1), exhibit significant swelling due to the osmotic pressure generated by counterions and salt ions. These ions are localized within the gel volume due to the Donnan equilibrium.[1−13] At equilibrium, corresponding to a free-standing gel, the osmotic pressure is counterbalanced by the stress generated in deformed polyelectrolyte strands. The gel swelling ability is quantified by the swelling ratio $Q = V/V_0$, demonstrating how much the volume of the gel, V, is changed with respect to that of a dry network, V_0. In salt-free aqueous solutions, polyelectrolyte gels could increase in volume by 100 times, Q~100.[2,7,8] Unfortunately, salt-free conditions are rare in practical applications where salt concentrations are relatively high, 0.1 − 1.0 M.[2,14,15] The presence of salt diminishes the osmotic effect of counterions, significantly limiting the polyelectrolyte gel's swelling capacity and reducing Q~20.[3−7,9−13] However, a strong dependence of gel swelling on salt concentration makes polyelectrolyte gels a mechano-chemical system capable of absorbing solvent which amount could be controlled by changing solution pH or salt concentration.[16−24] This feature of polyelectrolyte gels was exploited in the design of absorbing materials used in agriculture and consumer goods, drug delivery systems, implantable devices, 3D manufacturing, and water purification systems.[25−36]

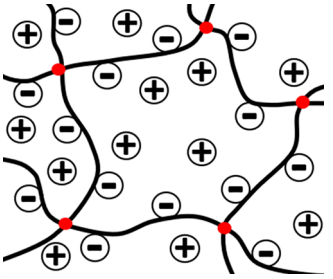

Figure 1. Schematic representation of a polyelectrolyte gel.

Although the passive response of polyelectrolyte gels to changes in environmental conditions has been extensively studied,[3,6,21,24,37−41] the effects of mechanical deformations on polyelectrolyte gel swelling were overlooked. To address this issue, we focus on how the biaxial deformation of a polyelectrolyte gel in contact with a salt solution could transform mechano-chemical equilibrium and affect salt and

Received: May 24, 2023
Revised: July 14, 2023
Published: August 1, 2023

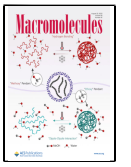

https://doi.org/10.1021/acs.macromol.3c01034
Macromolecules 2023, 56, 6543−6551

solvent partitioning in a gel in the framework of the Flory–Rehner approach.[42] This analysis reveals a nonmonotonic dependence of the gel swelling ratio on deformation. At high deformation levels, the polyelectrolyte gel contracts and expels salt, resulting in swelling below that of free-standing gels. To further understand the molecular basis of this process, we perform coarse-grained molecular dynamics simulations of polyelectrolyte gel deformation in contact with a salt solution.

The remaining part of the paper is organized as follows. We begin with adapting the Flory–Rehner model[16,17,42] of the nonlinear gel deformation to networks of charged polymers. After that, we present the results of coarse-grained molecular dynamics simulations of the biaxial deformation of a film made of crosslinked polyelectrolyte chains in contact with a salt solution. This simulation setup offers the advantage of simplifying the modeling of ion exchange between the surrounding solution and the swollen network. The film geometry of the charged gel allows us to study the redistribution of salt between the gel and surrounding solution in the entire range of polyelectrolyte gel deformations.

SWELLING AND DEFORMATION OF POLYELECTROLYTE GELS

Consider a network of polyelectrolyte chains with the degree of polymerization between crosslinks n_x and a fraction of ionizable groups f. The polyelectrolyte network is undergoing swelling and deformation in a salt solution with salt concentration (number density) ρ_s from a dry state with monomer number density ρ_0, initial dimensions $L_{0,i}$ (i = x, y, and z), and initial volume $V_0 = L_{0,x}L_{0,y}L_{0,z}$ reaching dimensions L_i and volume $V = L_xL_yL_z$ (Figure 2). The final

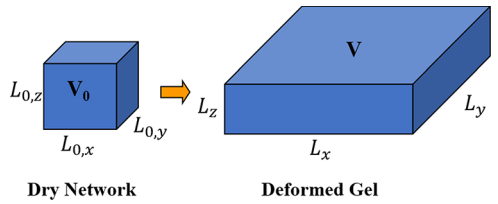

Figure 2. Swelling and deformation of a dry polyelectrolyte network in salt solution from volume V_0 to volume V.

state of the gel is characterized by the elongation $\lambda_i = L_i/L_{0,i}$ and swelling $Q = V/V_0$ ratios quantifying shape and volumetric changes with respect to a dry state. The total Helmholtz free energy of the swollen and deformed network surrounded by a salt solution is a sum

$$F_{total} = F_{elast}(\{L_i\}) + F_{gel}(V, \rho_g, \rho_{sol,g}, \rho_c, \rho_{s,g}^+, \rho_{s,g}^-) + F_{sol}(V_{sol}, \rho_{sol}, \rho_s) \quad (1)$$

of the elastic free energy of the gel, $F_{elast}(\{L_i\})$, free energy of the gel/solvent system, $F_{gel}(V, \rho_g, \rho_{sol,g}, \rho_c, \rho_{s,g}^+, \rho_{s,g}^-)$ describing the solvent, salt ion, and counterion distributions in a gel and interactions of monomers, solvent, counterions, positively and negatively charged salt ions with densities ρ_g, $\rho_{sol,g}$, ρ_c, $\rho_{s,g}^+$ and $\rho_{s,g}^-$, respectively, and free energy of the salt solution, $F_{sol}(V_{sol}, \rho_{sol}, \rho_s)$, occupying volume V_{sol} outside gel at a solvent ρ_{sol} and salt ρ_s densities. We assume that the total volume of the gel/salt solution system, V_{total}, does not change upon network swelling and deformation, $V_{total} = V + V_{sol}$ = constant.

In the framework of the Flory–Rehner approach,[16,17,42] the elastic free energy of a gel with semiflexible strands is written as follows:[43−45]

$$F_{elast}^{FR}(\{L_i\}) = \frac{1}{6}V_0G_{dr}I_1(1 + 2(1 - \beta I_1/3)^{-1}) \quad (2)$$

where $I_1 = \lambda_x^2 + \lambda_y^2 + \lambda_z^2$ is the first deformation invariant expressed in terms of the deformation ratios λ_i. There are two parameters in eq 2 that relate the network's deformation and swelling ability to its structure: (i) the strain-stiffening parameter (strand elongation ratio) β and (ii) the structural shear modulus in the dry state, G_{dr}. The parameter $\beta = \langle R_{in}^2\rangle/R_{max}^2$ is a ratio of the mean-square end-to-end distance of a network strand between crosslinks $\langle R_{in}^2\rangle$ in the undeformed network and the square of the end-to-end distance of a fully extended strand, $R_{max}^2 = n_x^2l^2$, with monomer projection length l and the degree of polymerization of network strands between crosslinks n_x. The structural modulus of a dry network with monomer number density ρ_0 made by crosslinking polyelectrolyte strands with the Kuhn length b_K is equal to[44−46]

$$G_{dr} = k_BTC\frac{\rho_0}{n_x}\frac{\langle R_{in}^2\rangle}{b_KR_{max}} \quad (3)$$

where C is a numerical constant that accounts for the network topology and crosslink functionality, k_B is the Boltzmann constant, and T is absolute temperature.

The true stress generated in the deformed gel under biaxial deformation in the xy-plane is equal to

$$\sigma_{xx} = \frac{1}{L_yL_z}\frac{\partial F_{total}}{\partial L_x} = \frac{V_0}{L_yL_z}\frac{L_x}{L_{0,x}^2}\frac{G_{dr}}{3}(1 + 2(1 - \beta I_1/3)^{-2}) + \frac{\partial F_{gel}(V, \rho_g, \rho_{s,g})}{\partial V} - \frac{\partial F_{sol}(V_{sol}, \rho_s)}{\partial V_{sol}} \quad (4)$$

A similar expression can be written down for the y-component of the stress tensor, σ_{yy}. Since no force is applied in the z-direction, we have

$$0 = \frac{1}{L_xL_y}\frac{\partial F_{total}}{\partial L_z} = \frac{V_0}{L_xL_y}\frac{L_z}{L_{0,z}^2}\frac{G_{dr}}{3}(1 + 2(1 - \beta I_1/3)^{-2}) + \frac{\partial F_{gel}(V, \rho_g, \rho_{sol,g})}{\partial V} - \frac{\partial F_{sol}(V_{sol}, \rho_{sol})}{\partial V_{sol}} \quad (5)$$

Equations 4 and 5 can be rewritten in terms of the deformation ratios λ_i, the swelling ratio of the gel Q and gel osmotic pressure

$$\pi(Q) = -\partial F_{gel}/\partial V + \partial F_{sol}/\partial V_{sol} \quad (6)$$

as follows

$$\sigma_{xx} = \frac{1}{3}G_{dr}\frac{\lambda_x}{\lambda_z\lambda_y}(1 + 2(1 - \beta I_1/3)^{-2}) - \pi(Q) \quad (7a)$$

$$0 = \frac{1}{3}G_{dr}\frac{\lambda_z}{\lambda_x\lambda_y}(1 + 2(1 - \beta I_1/3)^{-2}) - \pi(Q) \quad (7b)$$

Biaxially deformed gels are described by two independent variables λ and Q that reflect changes in the gel shape and occupied volume

https://doi.org/10.1021/acs.macromol.3c01034
Macromolecules 2023, 56, 6543−6551

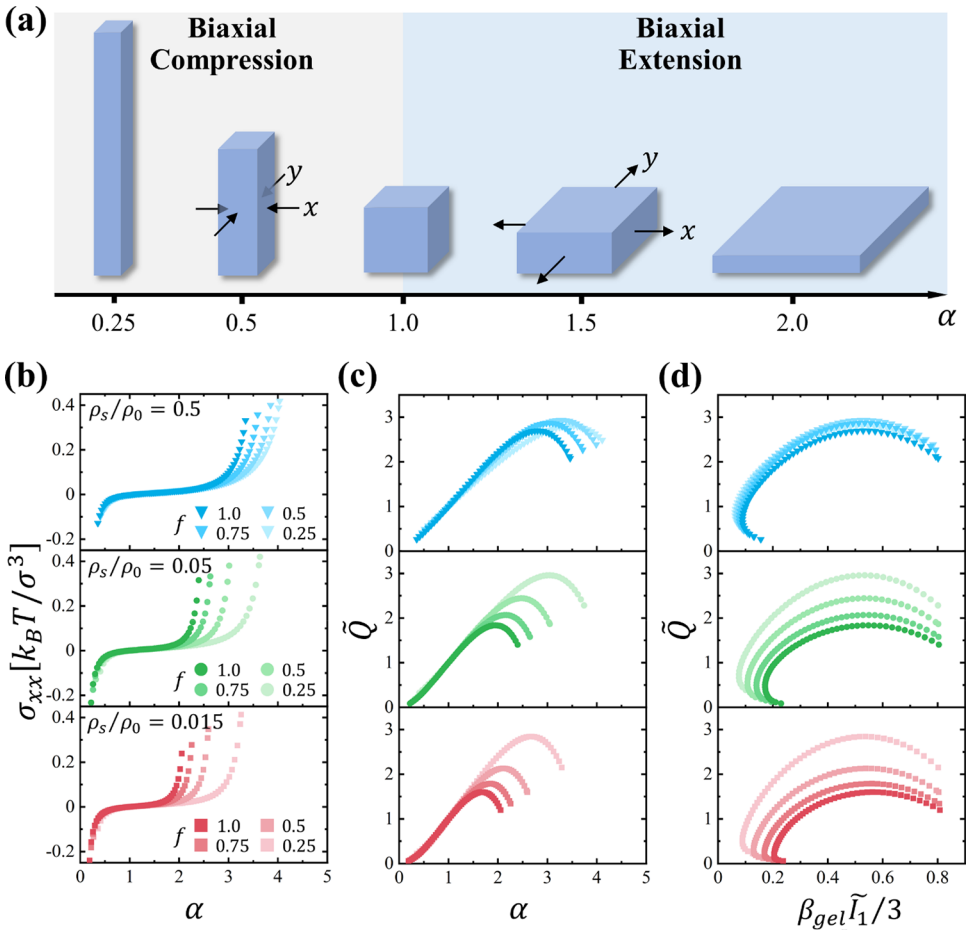

Figure 3. (a) Schematic representation of gel shape as a function of gel's deformation ratio α with respect to the equilibrium swollen state. Swelling and deformation of a polyelectrolyte network with structural modulus in the dry state G_{dr}=0.01 k_BT/σ^3 with monomer number density ρ_0 = 0.2 and β = 0.04 in salt solutions. Dependence of the biaxial stress σ_{xx} (b) and equilibrium gel swelling ratio $\tilde{Q} = Q/Q_{eq}^f$ (c) on deformation ratio α for polyelectrolyte gels with fraction of the ionized groups f equal to 0.25, 0.5, 0.75, and 1.0 (corresponding to the colors from light to dark) and different salt concentrations corresponding to ρ_s/ρ_0= 0.015 (squares), 0.05 (circles), and 0.5 (triangles). (d) Dependence of the gel swelling ratio $\tilde{Q}$ on $\beta_{gel}\tilde{I}_1/3$ for polyelectrolyte gels shown in panel b.

$$\lambda_x = \lambda_y = \lambda;\ Q = \lambda_x\lambda_y\lambda_z;\ \lambda_z = Q/\lambda^2;\ I_1 = 2\lambda^2 + Q^2/\lambda^4 \tag{8}$$

After taking into account relationships given by eq 8, eqs 7a and 7b are reduced to

$$\sigma_{xx} = \sigma_{yy} = \frac{1}{3}G_{dr}\left(\frac{\lambda^2}{Q} - \frac{Q}{\lambda^4}\right)(1 + 2(1 - \beta I_1/3)^{-2}) \tag{9a}$$

$$\frac{1}{3}G_{dr}\frac{Q}{\lambda^4}(1 + 2(1 - \beta I_1/3)^{-2}) = \pi(Q) \tag{9b}$$

For free-standing polyelectrolyte gels, $\sigma_{xx} = \sigma_{yy} = 0$, resulting in $\lambda_x = \lambda_y = \lambda_z = \lambda = Q^{1/3}$ (eq 9a) which transforms eq 9b into the classical Flory–Rehner expression defining the equilibrium gel swelling ratio, Q_{eq}^f, by balancing gel shear modulus and osmotic pressure.

Note that our selection of biaxial gel deformation is dictated by the setup of our coarse-grained molecular dynamics simulations of the polyelectrolyte gel swelling and deformation which is modeled as a gel slab surrounded by a salt solution. This setting allows for easy exchange of salt ions between the outside salt solution and gel's interior as it undergoes swelling and stretching as discussed below.

In polyelectrolyte gels, there are two contributions to osmotic pressure associated with a solvent quality for the uncharged polymer backbone and with a salt partitioning between the polyelectrolyte gel and the surrounding solvent. The ionic contribution to the osmotic pressure is accounted for by using Donnan's equilibrium condition for the ionic species.[47] Assuming a θ-solvent condition for the polymer backbone, the osmotic pressure of a polyelectrolyte gel has the following form

$$\pi(Q) = \frac{1}{3}k_BT\rho_0Q^{-3} + k_BT\left(\sqrt{(f\rho_0Q^{-1})^2 + 4\rho_s^2} - 2\rho_s\right) \tag{10}$$

In writing the ionic term of the osmotic pressure in eq 10, we assume that all counterions are "free" and contribute to the osmotic pressure.

Our analysis of the polyelectrolyte gel mechanics presented above considers a network dry state as a reference state. However, for polyelectrolyte gels, their mechanical properties in the dry state could be significantly different from those in the swollen state due to the association of ionizable groups playing a role of additional crosslinks. Therefore, it is convenient to rewrite eqs 9a and 9b by considering an equilibrium swelling state of a free-standing polyelectrolyte gel

https://doi.org/10.1021/acs.macromol.3c01034
Macromolecules 2023, 56, 6543−6551

with a swelling ratio Q_{eq}^{f} as a reference state. Defining the gel's deformation ratios α_i with respect to this state, we arrive at

$$\alpha_x = \alpha_y = \alpha = \lambda/Q_{eq}^{f\,1/3};\ \alpha_z = \tilde{Q}/\alpha^2;\ \tilde{Q} = Q/Q_{eq}^{f};$$
$$\tilde{I}_1 = (2\alpha^2 + \tilde{Q}^2/\alpha^4)$$

$$G_{gel} = G_{dr}/Q_{eq}^{f\,1/3};\ \beta_{gel} = \beta Q_{eq}^{f\,2/3} \tag{11}$$

In these new variables, eqs 9a and 9b are rewritten as follows

$$\sigma_{xx} = \sigma_{yy} = \frac{1}{3}G_{gel}\left(\frac{\alpha^2}{\tilde{Q}} - \frac{\tilde{Q}}{\alpha^4}\right)(1 + 2(1 - \beta_{gel}\tilde{I}_1/3)^{-2}) \tag{12a}$$

$$\frac{1}{3}G_{gel}\frac{\tilde{Q}}{\alpha^4}(1 + 2(1 - \beta_{gel}\tilde{I}_1/3)^{-2}) = \pi(Q) \tag{12b}$$

Figure 3 combines the results of the numerical solution of the eqs 12a and 12b with the osmotic pressure term given by eq 10 replotted in terms of relative deformation ratio α. Figure 3a illustrates gel shape evolution starting from the equilibrium swelling state described by Q_{eq}^{f} to highly asymmetric biaxial deformation. The dependence of stress upon the stretching of polyelectrolyte gels is shown in Figure 3b. All curves demonstrate a monotonic increase of the stress with gel deformation with a strong nonlinear response when individual strand deformation approaches the fully extended strand limit. The gel swelling ratio $\tilde{Q}$ is a nonmonotonic function of gel deformation (Figure 3c). It first increases with gel deformation and then begins to decrease. The decrease in $\tilde{Q}$ as in the case of gels of neutral polymers indicates that a gel begins to shrink upon deformation expelling a solvent in order to minimize strand elongation caused by a combination of stretching and swelling. The height of the maximum of $\tilde{Q}$ increases while its location moves to the right with decreasing the fraction of ionized groups f and increasing salt concentration, indicating a weakening of the osmotic effect of the salt ions and counterions on the equilibrium gel swelling ability. In addition, both these effects result in weaker pre-stretching of the gel strands upon equilibrium swelling, providing a larger deformation window before the gel strands reach the nonlinear deformation regime. To highlight the role of nonlinear strand deformation in such gel response, we plot the normalized swelling ratio $\tilde{Q}$ as a function of $\beta_{gel}\tilde{I}_1/3$ (Figure 3d). By representing gel deformation as $\beta_{gel}\tilde{I}_1/3$, we effectively plot the gel swelling ratio as a function of the ratio $\langle R^2(\alpha)\rangle/R_{max}^2$, which characterizes the degree of elongation of the network strands. These curves have a peculiar shape with a double value of $\tilde{Q}$ as a function of $\beta_{gel}\tilde{I}_1/3$ in the regime where biaxial extension changes to uniaxial extension (biaxial compression). This curve shape immediately follows from the definition of the first deformation invariant in terms of α and Q (eq 11).

COMPUTER SIMULATIONS OF POLYELECTROLYTE GELS

We performed molecular dynamics simulations of the deformation of the gel film immersed in salt solution (Figure 4). We use a coarse-grained representation of polymer gels and small ions by modeling them as beads interacting through the truncated-shifted (WCA) potential:

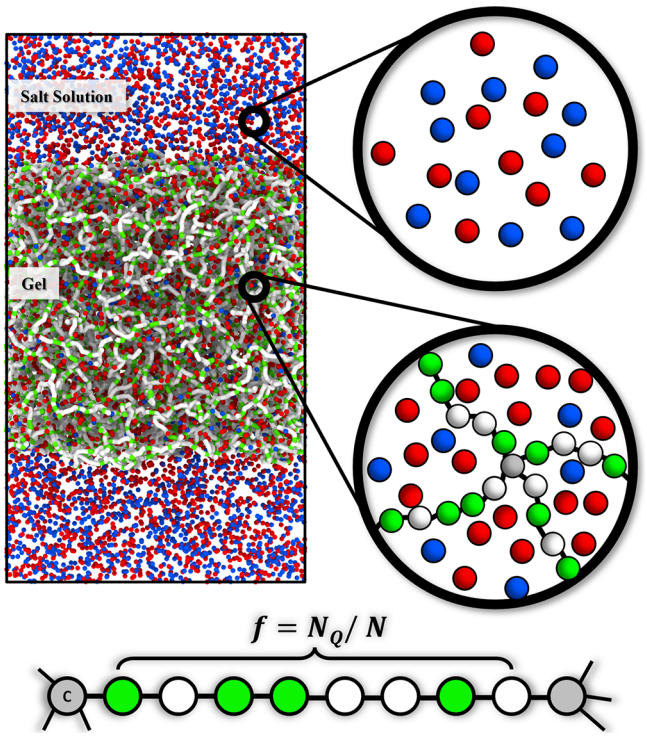

Figure 4. Snapshot of the simulation box containing a film of polyelectrolyte gels made of negatively charged strands surrounded by salt. Neutral beads on the polymer backbones are shown in white and negatively charged beads are colored in green. Positively and negatively charged ions are shown in red and blue colors, respectively. The inset on the bottom illustrates definition of the fraction of charged groups on gel strand with 8 beads. Crosslinker beads (gray) are not included in these calculations.

$$U_{LJ}(r) = \begin{cases} 4\varepsilon_{LJ}\left[\left(\frac{\sigma}{r}\right)^{12} - \left(\frac{\sigma}{r}\right)^{6} - \left(\frac{\sigma}{r_{cut}}\right)^{12} + \left(\frac{\sigma}{r_{cut}}\right)^{6}\right] & r < r_{cut} \\ 0 & r \geq r_{cut} \end{cases} \tag{13}$$

For all beads, the Lennard-Jones interaction parameter $\varepsilon_{LJ} = 1.0k_BT$ and the cutoff radius $r_{cut} = \sqrt[6]{2}\sigma$. The connectivity of beads into gel strands are modeled by a combination of the FENE potential:

$$U_{FENE}(r) = -\frac{1}{2}KR_0^2\ln\left(1 - \frac{r^2}{R_0^2}\right) \tag{14}$$

with the spring constant $K = 30k_BT\sigma^{-2}$ and the maximum bond length $R_0 = 1.5\ \sigma$, and pure repulsive WCA potential with $\varepsilon_{LJ} = 1.0\ k_BT$ and cutoff radius $r_{cut} = \sqrt[6]{2}\sigma$. The electrostatic interactions between charged beads with charge valences q_i and q_j separated by a distance r_{ij} are described by the Coulomb potential:

$$U_{Coul}(r_{ij}) = k_BTl_B\frac{q_iq_j}{r_{ij}} \tag{15}$$

https://doi.org/10.1021/acs.macromol.3c01034
Macromolecules 2023, 56, 6543−6551

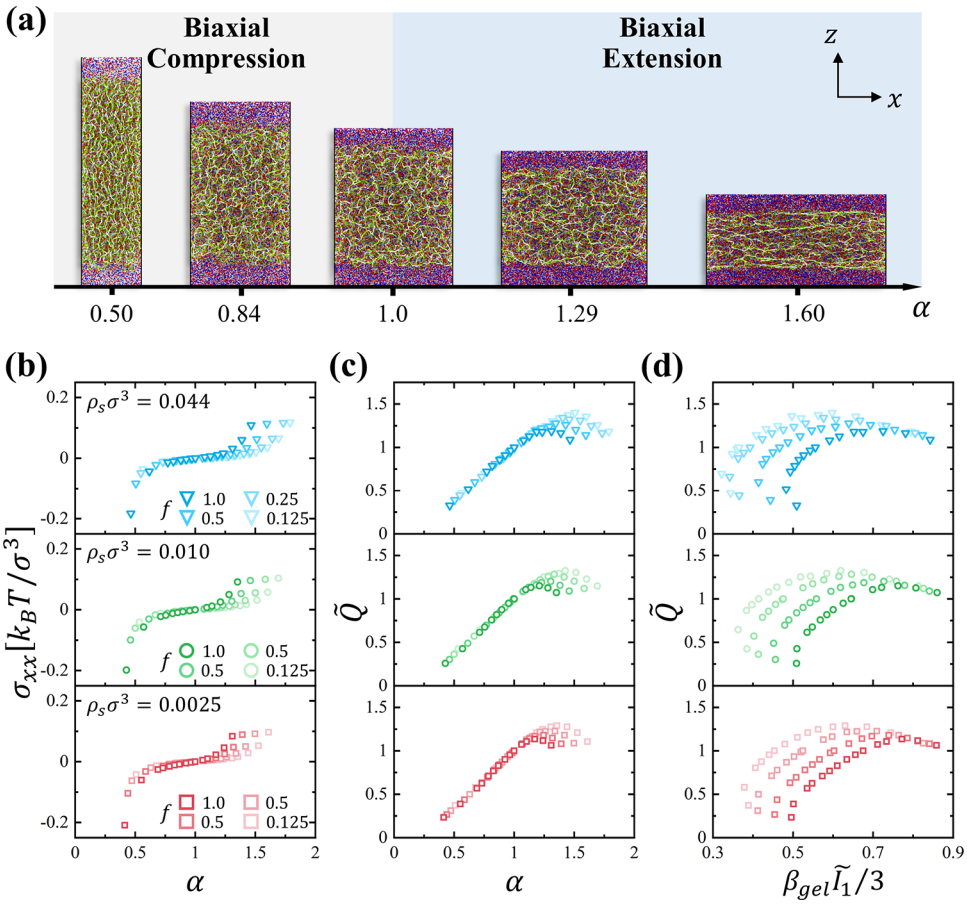

Figure 5. (a) Snapshots of gel shape as a function of gel's deformation ratio α with respect to the equilibrium swollen state. Dependence of the biaxial stress σ_{xx} (b) and equilibrium gel swelling ratio $\tilde{Q} = Q/Q_{eq}^{f}$ (c) on the deformation ratio α at different salt concentrations for polyelectrolyte gels with fraction of the ionized groups f equal to 0.125, 0.25, 0.5, and 1.0 shown by red, green, and blue symbols, respectively. (d) Dependence of the gel swelling ratio $\tilde{Q}$ on $\beta_{gel}\tilde{I}_1/3$ for polyelectrolyte gels is shown in panel b.

The Bjerrum length was set to $l_B = 1.0\ \sigma$ and charge valence was equal to $q_i = \pm 1$. The temperature was set to $T^* = 1.0\ k_BT/\varepsilon_{LJ}$.

The gel film was prepared by end-crosslinking chains with the degree of polymerization $N = 8$ to crosslinking beads uniformly distributed withing a film thickness (Figure 4). Each crosslinking bead is connected to four polymer chains. The film contains 1000 crosslinks and 2005 chains. The fraction of charged beads on the chain is varied between $f = 0.125$ and 1.0. The equilibrated film was placed in the middle of the simulation box which was filled with counterions and salt ions (Figure 4). Details of the network preparation and equilibration procedures are described in the Supporting Information. The simulations of gel deformation were performed under 3D periodic boundary conditions and a constant pressure in the z-direction. In particular, the stress–deformation curves in the swollen state were determined from a set of biaxial deformation simulations. In these simulations, a new deformed state was obtained by a series of small affine deformations $x_i \rightarrow (1 + \Delta\lambda)x_i$ and $y_i \rightarrow (1 + \Delta\lambda)y_i$ with a constant rate increment $\Delta\lambda = \nu t$ with $\nu = 0.01\sigma/\tau$ by maintaining pressure in the z direction constant at $P = P_{ext}$. The Nosé–Hoover style thermostat with time constant 5.0τ and barostat in the z-direction with external pressure set at P_{ext} and time constant 5.0τ, where $\tau = \sigma(m/\varepsilon_{LJ})^{1/2}$ is the standard Lennard-Jones time of beads with diameter σ, mass m, and the Lennard-Jones interaction parameter ε_{LJ}; the bead mass was set to unity in mass units for all beads. The velocity-Verlet algorithm with a time step $\Delta t = 0.005\tau$ was used for the integration of the beads' equations of motion. The electrostatic forces between charged beads were calculated by implementing the PPPM method with accuracy 10^{-4}. The P_{ext} value was selected in such to have a required salt concentration outside the gel by using the pressure/salt concentration calibration curve obtained from separate simulations of salt solutions (Figure S3). All simulations were performed using LAMMPS.[48]

In Figure 5, we illustrate how changes in salt concentration and fraction of the charged groups on gel strands influence gels' mechanical response. The data shown in Figure 5 are in very good agreement with predictions of a nonlinear version of the Flory–Rehner model of polyelectrolyte gel elasticity (Figure 3). Specifically, simulations confirm that with increasing the fraction of charged monomers f, the gel strands are more swollen, which shifts the crossover to the nonlinear gel deformation regime to smaller α-values (Figure 5b). The same trend continues for the dependence of normalized swelling ratio $\tilde{Q}$ on deformation α (Figure 5c) where the location of the maximum shifts toward smaller α-values while its magnitude is decreasing. The addition of salt reduces equilibrium gel swelling shifting the location of the maximum to larger α and increasing its magnitude (Figure 5c). Note, however, there are noticeable differences in $\tilde{Q}$ as a function of $\beta_{gel}\tilde{I}_1/3$ plots shown in Figures 3d and 5d. The theoretical plots

https://doi.org/10.1021/acs.macromol.3c01034
Macromolecules 2023, 56, 6543−6551

are more symmetric and round, while simulation data clearly show the change of curvature in the limit of large strand deformations. This is a manifestation of the excluded volume effects of counterions and salt ions at large gel deformations when the free volume available to small ions within a gel significantly diminishes (see Figure 5a). This effect is not included in our theoretical model.

To confirm that our model of nonlinear network elasticity correctly captures the gel elastic response in Figure 6a and to highlight the nonlinear effect in gel deformation, we plot the Mooney stress:[17]

$$G(\tilde{I}_1) \equiv \sigma_{yy}\left(\frac{\alpha^2}{\tilde{Q}} - \frac{\tilde{Q}}{\alpha^4}\right)^{-1} = \frac{1}{3}G_{gel}(1 + 2(1 - \beta_{gel}\tilde{I}_1/3)^{-2}) \quad (16)$$

as a function of $\tilde{I}_1/3$. The lines are the best fits to eq 16 by considering G_{gel} and β_{gel} as fitting parameters. The data are summarized in Table 1. Figure 6b combines all gel deformation data in one universal plot, confirming the validity of the functional form given by eq 16.

Figure 7a shows the dependence of polyelectrolyte gel structural modulus, G_{gel}, on the equilibrium gel density ρ_{gel} at different salt concentrations and fractions of the ionizable groups, f. The gel modulus monotonically decreases with increasing gel swelling (decreasing gel density), which is directly related with fraction of the ionizable groups on network strands. The data sets are clearly separated into two groups: one for lower salt concentrations ($\rho_s\sigma^3 \leq 0.01$) and another for high salt concentrations ($\rho_s\sigma^3 > 0.01$). Note that the gels in these groups with $f = 0.125$ and 0.25 could hardly be called polyelectrolyte gels since the network strands have one or two charges. The more pronounced effect of salt concentration on the gel swelling and shear modulus is observed for $\rho_s\sigma^3 > 0.01$. The grouping of these data sets could

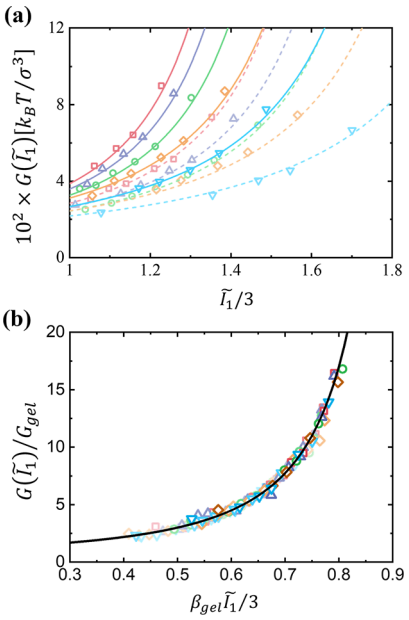

Figure 6. (a) Dependence of the Mooney stress on the first deformation invariant for swollen polyelectrolyte gels. The lines are the best fits to eq 16. (b) Normalized shear modulus $G(\tilde{I}_1)/G_{gel}$ as a function of $\beta_{gel}\tilde{I}_1/3$. Data and symbol notations are summarized in Table 1.

Table 1. Summary of Simulation Results

f	$\rho_s\sigma^3$	$\rho_{gel}\sigma^3$	G_{gel} $[k_BT/\sigma^3]$	G_0 $[k_BT/\sigma^3]$	β_{gel}	$\tilde{Q}_{max}$	α_{max}	Symbol
0.125	0.0025	0.086	0.0088	0.023	0.453	1.29	1.36	
0.25	0.0025	0.068	0.0087	0.028	0.524	1.23	1.34	
0.5	0.0025	0.054	0.0085	0.039	0.603	1.18	1.25	
1	0.0025	0.045	0.0084	0.056	0.675	1.14	1.17	
0.125	0.005	0.093	0.0088	0.021	0.433	1.32	1.34	
0.25	0.005	0.074	0.0087	0.026	0.501	1.25	1.30	
0.5	0.005	0.057	0.0086	0.036	0.583	1.19	1.27	
1	0.005	0.046	0.0085	0.053	0.663	1.14	1.19	
0.125	0.01	0.099	0.0089	0.020	0.414	1.32	1.43	
0.25	0.01	0.081	0.0088	0.024	0.475	1.28	1.33	
0.5	0.01	0.062	0.0087	0.033	0.558	1.20	1.31	
1	0.01	0.049	0.0086	0.048	0.645	1.15	1.21	
0.125	0.023	0.110	0.0102	0.022	0.389	1.36	1.48	
0.25	0.023	0.092	0.0099	0.024	0.442	1.31	1.39	
0.5	0.023	0.072	0.0098	0.031	0.516	1.22	1.29	
1	0.023	0.056	0.0095	0.044	0.603	1.16	1.19	
0.125	0.044	0.116	0.0105	0.021	0.365	1.40	1.51	
0.25	0.044	0.103	0.0102	0.022	0.392	1.34	1.40	
0.5	0.044	0.082	0.0100	0.027	0.466	1.28	1.34	
1	0.044	0.063	0.0097	0.036	0.556	1.19	1.31	

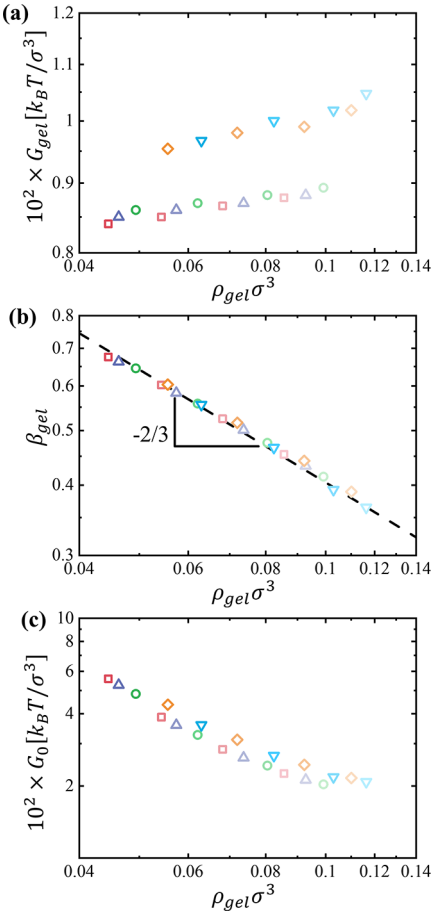

Figure 7. (a) Dependence of gel modulus G_{gel} on equilibrium gel density ρ_{gel} for different salt concentrations and fraction of the ionized groups f. (b) Gel extensibility ratio β_{gel} as a function of ρ_{gel}. (c) Dependence of gel modulus G_0 at small deformations on equilibrium gel density ρ_{gel}. Symbol notations are summarized in Table 1.

https://doi.org/10.1021/acs.macromol.3c01034
Macromolecules 2023, 56, 6543−6551

indicate the onset of counterion condensation with increasing salt concentration. As expected, the addition of salt results in the decrease in gel swelling ability and an increase in gel modulus. The gel extensibility ratio β_{gel} (Figure 7b) monotonically increases with decreasing gel density indicating a strong prestretching of the gel strand at equilibrium swelling. All data sets collapse into a universal curve described by the scaling relation $\beta_{gel} \sim \rho_{gel}^{-2/3}$, in accordance with eq 11.

The shear modulus of polyelectrolyte gels at small deformations

$$G_0 \equiv \frac{1}{3} G_{gel}(1 + 2(1 - \beta_{gel})^{-2}) \tag{17}$$

depends on both the structural shear modulus G_{gel} and extensibility ratio β_{gel}. The combined effect of these two parameters results in a monotonic decrease of the shear modulus G_0 with gel density ρ_{gel} (Figure 7c). This unexpected modulus dependence is due to the dominant contribution to gel elasticity by the finite strand extensibility associated with the divergent term in eq 17. Thus, the modeled polyelectrolyte gels achieve equilibrium swelling in the limit of large strand elongations.

Figure 8a,b shows the evolution of charge distribution across the simulation box with increasing gel deformation. Specifically, Figure 8a shows dependence of the ion density within a gel on the gel deformation. The magnitude of positive ion density decreases with increasing the deformation ratio α. Note that the net charge of the gel is zero, which is confirmed by the overlap of the density profiles of positive and negative charges combined in Figure 8b. At large deformation, $\alpha = 1.305$, there is structuring in charge distribution on the polymer backbones due to the strong alignment of the network strands imposed by the strand packing constraints.

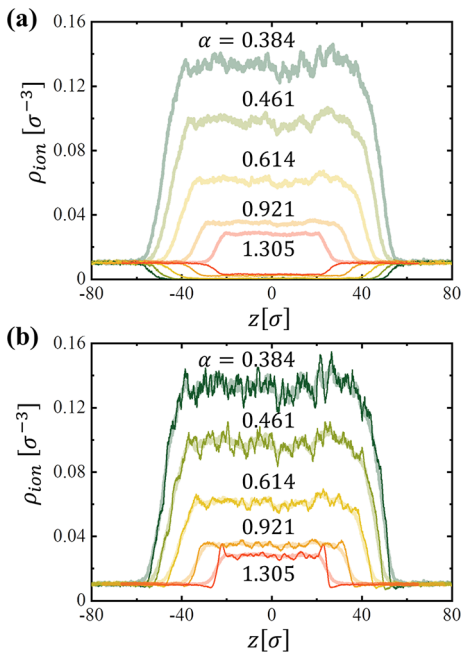

Figure 8. (a) Density profiles of positively charged salt ions and counterions (thick lines) and negatively charged salt ions (thin lines) along the z direction for different deformation ratios α = 0.384,0.461,0.614,0.921,1.305 of gels with $f = 0.5$ in a solution with bulk salt concentration $\rho_s = 0.01\sigma^{-3}$. (b) Density profiles of positive charges (thick lines) and negative charges including charges on the network strands (thin lines) along the z-direction for the data sets are shown in panel a.

CONCLUSIONS

We utilize a combination of analytical calculations and molecular dynamics simulations to investigate the biaxial nonlinear deformation of polyelectrolyte gels in salt solutions as a function of the fraction of ionizable groups on the network strands and salt concentrations. The results from both theory and simulations reveal that polyelectrolyte gels undergo deswelling with increasing deformation. This process is driven by the optimization of the stretching of the network strands and osmotic pressure of the counterions and salt ions (Figures 3 and 5). The crossover point to the deswelling regime shifts to the smaller deformation ratios α with decreasing salt concentration and increasing fraction of the ionizable groups on network strands. Note that this deswelling behavior mirrors that observed in brush gels under uniaxial deformation.[49] Our analysis of the gel deformation (Figure 6) shows that the gel nonlinear elastic response is well described by a model based on the nonlinear deformation of semiflexible strands with a characteristic quadratic divergence of stress at large deformations (eqs 9a and 9b). The gel extensibility ratio β_{gel}, which governs the network nonlinear response, scales with gel density as $\beta_{gel} \propto \rho_{gel}^{-2/3}$. This scaling relation is in very good agreement with the nonlinear gel deformation model (eq 11).

The developed framework to study polyelectrolyte gel swelling and deformation is different from the currently adopted approach. Instead of using hybrid of molecular dynamics simulations and Monte Carlo simulations for ion exchange between a gel and a salt reservoir,[38,50−52] we performed simulations of the gel film surrounded by salt solution. This setup has an advantage since it does not suffer from simulation slow down due to the rejection of insertion steps at large densities of salt ions and monomers in a gel. For the first time we studied polyelectrolyte gel deformations in the linear and nonlinear deformation regimes. Our model of the nonlinear gel elasticity is based on the expression for deformation of the semiflexible strands,[53,54] which is more realistic in describing large deformations of different network systems[43,54−58] than a network model based on deformation of the freely jointed strands.[17,20,38,59]

Our approach can be extended to examine the effects of gel deformation on the dissociation equilibrium of ionizable groups in gels of weak polyelectrolytes.[50,52,59,60] Such a study could illuminate the interplay between solution pH and nonlinear gel elasticity. We hope that this work will prompt further studies in this area.

ASSOCIATED CONTENT

Supporting Information

The Supporting Information is available free of charge at https://pubs.acs.org/doi/10.1021/acs.macromol.3c01034.

Computer simulation details, equilibration of the polyelectrolyte gel films in salt solutions, concentration dependence of the pressure in salt solutions, and time evolution of the PE gel density during production runs (PDF)

https://doi.org/10.1021/acs.macromol.3c01034
Macromolecules 2023, 56, 6543−6551

AUTHOR INFORMATION

Corresponding Author

Andrey V. Dobrynin − *Department of Chemistry, University of North Carolina, Chapel Hill, North Carolina 27599-3290, United States;* orcid.org/0000-0002-6484-7409; Email: avd@email.unc.edu

Authors

Zilu Wang − *Department of Chemistry, University of North Carolina, Chapel Hill, North Carolina 27599-3290, United States;* orcid.org/0000-0002-5957-8064

Yuan Tian − *Department of Chemistry, University of North Carolina, Chapel Hill, North Carolina 27599-3290, United States;* orcid.org/0000-0002-7277-1408

Complete contact information is available at: https://pubs.acs.org/10.1021/acs.macromol.3c01034

Notes

The authors declare no competing financial interest.

ACKNOWLEDGMENTS

This work was supported by the National Science Foundation under the grant DMR 2049518.

REFERENCES

(1) Dobrynin, A. V. Theory and Simulations of Charged Polymers: From Solution Properties to Polymeric Nanomaterials. *Curr. Opin. Colloid Interface Sci.* **2008**, *13*, 376−388.

(2) Horkay, F.; Tasaki, I.; Basser, P. J. Osmotic Swelling of Polyacrylate Hydrogels in Physiological Salt Solutions. *Biomacromolecules* **2000**, *1*, 84−90.

(3) Katchalsky, A.; Michaeli, I. Polyelectrolyte Gels in Salt Solutions. *J. Polym. Sci.* **1955**, *15*, 69−86.

(4) Longo, G. S.; Olvera de la Cruz, M.; Szleifer, I. Molecular Theory of Weak Polyelectrolyte Gels: The Role of pH and Salt Concentration. *Macromolecules* **2011**, *44*, 147−158.

(5) Mann, B. A.; Holm, C.; Kremer, K. Swelling of Polyelectrolyte Networks. *J. Chem. Phys.* **2005**, *122*, 154903.

(6) Rubinstein, M.; Colby, R. H.; Dobrynin, A. V.; Joanny, J.-F. Elastic Modulus and Equilibrium Swelling of Polyelectrolyte Gels. *Macromolecules* **1996**, *29*, 398−406.

(7) Yin, D.-W.; Olvera de la Cruz, M.; de Pablo, J. J. Swelling and Collapse of Polyelectrolyte Gels in Equilibrium with Monovalent and Divalent Electrolyte Solutions. *J. Chem. Phys.* **2009**, *131*, 194907.

(8) Mann, B. A.; Kremer, K.; Holm, C. The Swelling Behavior of Charged Hydrogels. *Macromol. Symp.* **2006**, *237*, 90−107.

(9) Dobrynin, A. V., Polyelectrolyte Solutions and Gels. In *The Oxford Handbook of Soft Condensed Matter*, Terentjev, E. M.; Weitz, D. A., Eds.; Oxford University Press: Oxford, 2015; pp 383−450.

(10) Dobrynin, A. V. Polyelectrolytes: On the Doorsteps of the Second Century. *Polymer* **2020**, *202*, No. 122714.

(11) Dobrynin, A. V.; Colby, R. H.; Rubinstein, M. Scaling Theory of Polyelectrolyte Solutions. *Macromolecules* **1995**, *28*, 1859−1871.

(12) Ilavský, M. Effect of Electrostatic Interactions on Phase Transition in the Swollen Polymeric Network. *Polymer* **1981**, *22*, 1687−1691.

(13) Khare, A. R.; Peppas, N. A. Swelling/Deswelling of Anionic Copolymer Gels. *Biomaterials* **1995**, *16*, 559−567.

(14) Kazanskii, K. S.; Dubrovskii, S. A. Chemistry and Physics of "Agricultural" Hydrogels. In *Polyelectrolytes Hydrogels Chromatographic Materials*; Springer Berlin: Heidelberg, 1992; pp 97−133.

(15) Peppas, N. A.; Bures, P.; Leobandung, W.; Ichikawa, H. Hydrogels in Pharmaceutical Formulations. *Eur. J. Pharm. Biopharm.* **2000**, *50*, 27−46.

(16) Flory, P. J. *Principles of Polymer Chemistry*; Cornell University Press: Ithaca, NY, 1971.

(17) Treloar, L. R. G. *The Physics of Rubber Elasticity*; Clarendon Press: Oxford, 1975.

(18) McKenna, G. B. Soft matter: rubber and networks. *Rep. Prog. Phys.* **2018**, *81*, No. 0666602.

(19) Peppas, N. A.; Hilt, J. Z.; Khademhosseini, A.; Langer, R. Hydrogels in biology and medicine: from molecular principles to bionanotechnology. *Adv. Mater.* **2006**, *18*, 1345−1360.

(20) Rubinstein, M.; Colby, R. H. *Polymer Physics*; Oxford University Press: New York, NY, 2003.

(21) Horkay, F.; McKenna, G. B., Polymer Networks and Gels. In *Physical Properties of Polymers Handbook*, Mark, J. E., Ed.; Springer: New York, NY, 2007; pp 497−523.

(22) Kuhn, W.; Hargitay, B.; Katchalsky, A.; Eisenberg, H. Reversible dilation and contraction by changing the state of ionization of high-polymer acid networks. *Nature* **1950**, *165*, 514−516.

(23) Katchalsky, A.; Eisenberg, H. Polyvinylphosphate contractile systems. *Nature* **1950**, *166*, 267−268.

(24) Katchalsky, A. Solutions of polyelectrolytes and mechanochemical systems. *J. Polym. Sci.* **1951**, *7*, 393−412.

(25) Wichterle, O.; Lim, D. Hydrophilic gels for biological use. *Nature* **1960**, *185*, 117−118.

(26) Buchholz, F. L.; Graham, A. T., *Modern superabsorbent polymer technology*; Wiley - VCH: New York, 1998.

(27) Brannon-Peppas, L.; Harland, R. S. Absorbent polymer technology. *J. Controlled Release* **1991**, *17*, 297−298.

(28) Debashish, R.; Cambre, J. N.; Sumerlin, B. S. Future perspectives and recent advances in stimuli-responsive materials. *Prog. Polym. Sci.* **2010**, *35*, 278−301.

(29) Hoffman, A. S. Hydrogels for biomedical applications. *Adv. Drug Delivery Rev.* **2002**, *64*, 18−23.

(30) Guilherme, M. R.; Aouada, F. A.; Fajardo, A. R.; Martins, A. F.; Paulino, A. T.; Davi, M. F. T.; Rubira, A. F.; Muniz, E. C. Superabsorbent hydrogels based on polysaccharides for application in agriculture as soil conditioner and nutrient carrier: A review. *Eur. Polym. J.* **2015**, *72*, 365−385.

(31) Zhang, Y.; Chan, H. F.; Leong, K. W. Advanced materials and processing for drug delivery: the past and the future. *Adv. Drug Delivery Rev.* **2013**, *65*, 104−120.

(32) Shaviv, A. Advances in controlled-release fertilizers. *Adv. Agron.* **2001**, *71*, 1−49.

(33) Zhang, Y. S.; Khademhosseini, A. Advances in engineering hydrogels. *Science* **2017**, *356*, No. eaaf3627.

(34) Guo, Y.; Bae, J.; Fang, Z.; Li, P.; Zhao, F.; Yu, G. Hydrogels and Hydrogel-Derived Materials for Energy and Water Sustainability. *Chem. Rev.* **2020**, *120*, 7642−7707.

(35) Ligon, S. C.; Liska, R.; Stampfl, J.; Gurr, M.; Mülhaupt, R. Polymers for 3D Printing and Customized Additive Manufacturing. *Chem. Rev.* **2017**, *117*, 10212−10290.

(36) Kazanskii, K. S.; Dubrovskii, S. A. Chemistry and physics of agricultural hydrogels. *Adv. Polym. Sci.* **1992**, *104*, 97−133.

(37) Harland, R.; Prud'homme, R. *Polyelectrolyte Gels*; American Chemical Society: Washington, DC, 1992.

(38) Kosovan, P.; Richter, T.; Holm, C. Modeling polyelectrolyte gels in equilibrium with salt solutions. *Macromolecules* **2015**, *48*, 7698−7708.

(39) Khokhlov, A. R.; Starodubtzev, S. G.; Vasilevskaya, V. V. Conformational Transitions in Polymer Gels - Theory and Experiment. *Adv. Polym. Sci.* **1993**, *109*, 123−175.

(40) Edgecombe, S.; Schneider, S.; Linse, P. Monte Carlo Simulations of Defect-Free Cross-Linked Gels in the Presence of Salt. *Macromolecules* **2004**, *37*, 10089−10100.

(41) Rud, O.; Richter, T.; Borisov, O.; Holm, C.; Košovan, P. A selfconsistent mean-field model for polyelectrolyte gels. *Soft Matter* **2017**, *13*, 3264−3274.

(42) Flory, P. J.; Rehner, J. Statistical mechanics of cross-linked polymer networks II. Swelling. *J. Chem. Phys.* **1943**, *11*, 521−526.

(43) Dobrynin, A. V.; Carrillo, J.-M. Y. Universality in nonlinear elasticity of biological and polymeric networks and gels. *Macromolecules* **2011**, *44*, 140−146.

(44) Jacobs, M.; Liang, H.; Dashtimoghadam, E.; Morgan, B. J.; Sheiko, S. S.; Dobrynin, A. V. Nonlinear Elasticity and Swelling of Comb and Bottlebrush Networks. *Macromolecules* **2019**, *52*, 5095−5101.
(45) Jacobs, M.; Vashahi, F.; Maw, M.; Sheiko, S. S.; Dobrynin, A. V. Brush gels: Where theory, simulations and experiments meet. *Macromolecules* **2022**, *55*, 7922−7931.
(46) Liang, H.; Sheiko, S. S.; Dobrynin, A. V. Supersoft and Hyperelastic Polymer Networks with Brushlike Strands. *Macromolecules* **2018**, *51*, 638−645.
(47) Donnan, F. G. The Theory of Membrane Equilibria. *Chem. Rev.* **1924**, *1*, 73−90.
(48) Thompson, A. P.; Aktulga, H. M.; Berger, R.; Bolintineanu, D. S.; Brown, W. M.; Crozier, P. S.; in't Veld, P. J.; Kohlmeyer, A.; Moore, S. G.; Nguyen, T. D.; Shan, R.; Stevens, M. J.; Tranchida, J.; Trott, C.; Plimpton, S. J. LAMMPS - a flexible simulation tool for particle-based materials modeling at the atomic, meso, and continuum scales. *Comput. Phys. Commun.* **2022**, *271*, No. 108171.
(49) Jacobs, M.; Tian, Y.; Dobrynin, A. V. Deformation driven deswelling of brush gels. *Macromolecules* **2023**, *56*, 2209−2216.
(50) Landsgesell, J.; Nova, L.; Rud, O.; Uhlik, F.; Sean, D.; Hebbeker, P.; Holm, C.; Košovan, P. Simulations of ionization equilibria in weak polyelectrolyte solutions and gels. *Soft Matter* **2019**, *15*, 1155−1185.
(51) Landsgesell, J.; Hebbeker, P.; Rud, O.; Lunkad, R.; Kosovan, P.; Holm, C. Grand-Reaction Method for Simulations of Ionization Equilibria Coupled to Ion Partitioning. *Macromolecules* **2020**, *53*, 3007−3020.
(52) Beyer, D.; Kosovan, P.; Holm, C. Simulation explain the swelling behavior of hydrogeks with alternating neutral and weakly acidic blocks. *Macromolecules* **2022**, *55*, 10751−10760.
(53) Dobrynin, A. V.; Carrillo, J. M. Y.; Rubinstein, M. Chains are more flexible under tension. *Macromolecules* **2010**, *43*, 9181−9190.
(54) Carrillo, J.-M. Y.; MacKintosh, F. C.; Dobrynin, A. V. Nonlinear elasticity: from single chain to networks and gels. *Macromolecules* **2013**, *46*, 3679−3692.
(55) Sheiko, S. S.; Dobrynin, A. V. Architectural code for rubber elasticity: From supersoft to superfirm materials. *Macromolecules* **2019**, *52*, 7531−7546.
(56) Vatankhah-Varnosfaderani, M.; Daniel, W. F. M.; Everhart, M. H.; Pandya, A. A.; Liang, H. Y.; Matyjaszewski, K.; Dobrynin, A. V.; Sheiko, S. S. Mimicking biological stress-strain behaviour with synthetic elastomers. *Nature* **2017**, *549*, 497−501.
(57) Vatankhah-Varnosfaderani, M.; Keith, A. N.; Cong, Y. D.; Liang, H. Y.; Rosenthal, M.; Sztucki, M.; Clair, C.; Magonov, S.; Ivanov, D. A.; Dobrynin, A. V.; Sheiko, S. S. Chameleon-like elastomers with molecularly encoded strain-adaptive stiffening and coloration. *Science* **2018**, *359*, 1509−1513.
(58) Jacobs, M.; Liang, H.; Dobrynin, A. V. Theory and simulations of hybrid networks. *Macromolecules* **2021**, *54*, 7337−7346.
(59) Landsgesell, J.; Beyer, D.; Hebbeker, P.; Kosovan, P.; Holm, C. The pH-Dependent Swelling of Weak Polyelectrolyte Hydrogels Modeled at Different Levels of Resolution. *Macromolecules* **2022**, *55*, 3176−3188.
(60) Longo, G. S.; de la Cruz, M. O.; Szleifer, I. Non-monotonic swelling of surface grafted hydrogels induced by pH and/or salt concentration. *J. Chem. Phys.* **2014**, *141*, 124909.

https://doi.org/10.1021/acs.macromol.3c01034
Macromolecules 2023, 56, 6543−6551